





RESEARCH ARTICLE

Overcoming presynaptic effects of VAMP2 mutations with 4-aminopyridine treatment

Roxanne L. Simmons¹ | Haiyan Li² | Baris Alten³ | Magda S. Santos² | Ruiji Jiang¹ | Brianna Paul¹ | Sanam J. Lalani¹ | Audrey Cortesi¹ | Kendall Parks¹ | Nitin Khandelwal⁴ | Bethany Smith-Packard⁵ | Malay A. Phoong⁶ | Michael Chez⁷ | Heather Fisher⁸ | Angela E. Scheuerle⁹ | Marwan Shinawi¹⁰  | Shaun A. Hussain¹¹ | Ege T. Kavalali³ | Elliott H. Sherr¹ | Susan M. Voglmaier² 

¹Department of Neurology, Weill Institute for Neurosciences and Institute of Human Genetics, School of Medicine, University of California, San Francisco, San Francisco, California, USA

²Department of Psychiatry, Weill Institute for Neurosciences and Kavli Institute for Fundamental Neuroscience, School of Medicine, University of California, San Francisco, San Francisco, California, USA

³Department of Pharmacology and Vanderbilt Brain Institute, Vanderbilt University, Nashville, Tennessee, USA

⁴Department of Neuroscience, UT Southwestern Medical Center, Dallas, Texas, USA

⁵Department of Pediatrics, Penn State Health Pediatric Specialties, Hershey, Pennsylvania, USA

⁶Division of Neuroscience, Department of Pediatric Neuropsychology, Sutter Medical Foundation, Sacramento, California, USA

⁷Neuroscience Medical Group, Sutter Medical Foundation, Sacramento, California, USA

⁸Department of Genetics, Children's Medical Center of Texas, Dallas, Texas, USA

⁹Division of Genetics and Metabolism, Department of Pediatrics, UT Southwestern Medical Center, Dallas, Texas, USA

¹⁰Division of Genetics and Genomic Medicine, St. Louis Children's Hospital, Washington University School of Medicine, St. Louis, Missouri, USA

¹¹Department of Pediatrics, UCLA Mattel Children's Hospital and Geffen School of Medicine, Los Angeles, California, USA

Correspondence

Elliott H. Sherr, Department of Neurology, Weill Institute for Neurosciences, School of Medicine, University of California, San Francisco, 675 Nelson Rising Ln, 214B, San Francisco, CA 94158, USA.
Email: Elliott.Sherr@ucsf.edu

Susan M. Voglmaier, Department of Psychiatry, Weill Institute for Neurosciences, School of Medicine, University of California, San Francisco, 401 Parnassus Ave, San Francisco, CA 94143, USA.
Email: Susan.Voglmaier@ucsf.edu

Funding information

National Institute of Neurological Disorders and Stroke, Grant/Award Number: NS058721; National Institute of Mental Health, Grant/Award Numbers: MH066198, MH083691

Abstract

Clinical and genetic features of five unrelated patients with *de novo* pathogenic variants in the synaptic vesicle-associated membrane protein 2 (VAMP2) reveal common features of global developmental delay, autistic tendencies, behavioral disturbances, and a higher propensity to develop epilepsy. For one patient, a cognitively impaired adolescent with a *de novo* stop-gain VAMP2 mutation, we tested a potential treatment strategy, enhancing neurotransmission by prolonging action potentials with the aminopyridine family of potassium channel blockers, 4-aminopyridine and 3,4-diaminopyridine, in vitro and in vivo. Synaptic vesicle recycling and neurotransmission were assayed in neurons expressing three VAMP2 variants by live-cell imaging and electrophysiology. In cellular models, two variants decrease both the rate of exocytosis and the number of synaptic vesicles released from the recycling pool, compared with wild-type. Aminopyridine treatment increases the rate and extent of exocytosis and total synaptic charge transfer and desynchronizes GABA release. The clinical response of the patient to 2 years of

off-label aminopyridine treatment includes improved emotional and behavioral regulation by parental report, and objective improvement in standardized cognitive measures. Aminopyridine treatment may extend to patients with pathogenic variants in VAMP2 and other genes influencing presynaptic function or GABAergic tone, and tested in vitro before treatment.

KEYWORDS

aminopyridine, neurodevelopmental disorder, synaptic transmission, synaptic vesicle, VAMP2

1 | INTRODUCTION

Fast communication between neurons relies on the precise and highly regulated fusion of synaptic vesicles (SVs) with the presynaptic plasma membrane, resulting in neurotransmitter exocytosis (Sudhof, 2013). Fusion of the two membranes is driven by the zippering of highly conserved hydrophobic side chain soluble *N*-ethylmaleimide-sensitive factor attachment protein receptor (SNARE) motifs of the vesicular v-SNARE, vesicle-associated membrane protein (VAMP2; MIM #185881) with the plasma membrane target t-SNAREs, SNAP-25, and syntaxin-1, to form the SNARE complex (Jahn & Scheller, 2006). The SNARE complex interacts with accessory proteins, such as the synaptotagmin family of Ca²⁺ sensors. Synaptotagmins sense the local increase in Ca²⁺ concentration caused by the opening of voltage-gated Ca²⁺ channels (VGCCs) upon action potential (AP)-induced membrane depolarization. The resultant local increase in Ca²⁺ concentration is signaled to the SNARE complex mainly by synaptotagmin-1 for synchronous release and by synaptotagmin-7 for asynchronous release. Simultaneously, inward-rectifier K⁺ channels and the Na⁺/K⁺-ATPase repolarizes the membrane, halting VGCC activity, while active pumps clear local Ca²⁺ away, terminating neurotransmitter release. VAMP2 is also vital for the fast endocytosis of neuronal membrane to replenish the pool of SVs for the next round of exocytosis (Deak, Schoch, Liu, Sudhof, & Kavalali, 2004).

VAMP2 is the most abundant SV protein, with approximately 70 copies per vesicle, while only 2–3 are necessary to mediate fusion (Mohrman & Sorensen, 2012; Takamori et al., 2006). Given the high conservation of the SNARE motif (Fasshauer, Eliason, Brunger, & Jahn, 1998), a mutation in this region would be expected to disrupt endocytosis or exocytosis of SVs, impairing neurotransmission and causing neurological disorders. Indeed, experimental SNARE mutations cause dominant negative disruption of fusion (Grote & Kelly, 1996; Koo et al., 2011), while VAMP2 heterozygosity loss of function in mice causes only a mild phenotype (Monteggia, Lin, Adachi, & Kavalali, 2018). Human VAMP2 SNARE mutations can impair fusion of reconstituted membranes. A clinical phenotype for VAMP2 mutations was recently described in five patients as hypotonia, intellectual disability, and autistic features (MIM #618760; Salpietro et al., 2019). Here we report five unrelated patients, doubling the number identified with pathogenic *de novo* VAMP2 variants. Currently, there is no effective treatment targeting the underlying impairment of

neurotransmitter release. Patients likely make wild-type (WT) VAMP2 from their functional allele, so we tested a strategy to overcome exocytosis defects by prolonging the AP by delaying neuronal repolarization with the potassium channel inhibitors 4-aminopyridine (4-AP) and 3,4-diaminopyridine (DAP) to increase calcium entry and SV release probability. 4-AP and DAP have expanding roles in the treatment of multiple sclerosis, cerebellar ataxias, and Lambert-Eaton and congenital myasthenic syndromes (Claassen, Teufel, Kalla, Spiegel, & Strupp, 2013; Palace, Wiles, & Newsom-Davis, 1991; Strupp et al., 2017). Taken together, this suggests an enhancement of SV release could improve cognitive function in patients with single allele VAMP2 pathogenic variants.

2 | METHODS

2.1 | Editorial policies and ethical considerations

Work with animals was conducted under the supervision of the Institutional Care and Use Committees of the University of California, San Francisco and Vanderbilt University Medical Center. Parents provided written consent before participation through a University of California, San Francisco (UCSF) committee on human research approved protocol.

2.2 | Clinical information

Patients with VAMP2 variants were assessed by chart review and caretaker phone interviews. Parents provided written consent before participation. Variants were assessed for clinical significance and pathogenicity by use of web sources including clinical data obtained from GeneDx, as well as predicted results from ClinVar, Poly-Phen2, and gnomAD. Thus, while variants of these patients were initially reported by GeneDx as “uncertain significance,” they were determined to be pathogenic based on clinical phenotype and predictive algorithms. Ancillary studies, including electroencephalography (EEG), electromyography, magnetic resonance imaging (MRI), and neuropsychologic testing were reviewed by a physician to determine clinical relevance. After receiving consent from parents and the patient, Patient 1 was treated with low dose 4-AP that was gradually increased over the course of several months. Tolerability of 4-AP was

assessed by parental report of worsening anxiety or insomnia. The effects of 4-AP were measured by qualitative assessments via subjective parental reports, and quantitatively via neuropsychological testing. Neuropsychological testing pre- and posttreatment were compared by converting scaled scores to Z-scores.

2.3 | Molecular biology and lentivirus preparation

VAMP2-mOrange2 (mOr2) fusions were constructed by fusing synthetic mOr2 (Shaner et al., 2008) to the C-terminus of human WT (RefSeq NM_014232.3) or variant VAMP2 complementary DNAs (cDNAs) with a linker (SGGSGGTG). Disease-associated point mutations Arg56Leu (R56L) or Gly73Trp (G73W) were generated in VAMP2 using Quikchange-XL2 Site-Directed Mutagenesis (Agilent) using the following primer pairs: For Arg56Leu: 5'-GACAACCTTC TGGTCCAGCTCCAGGACCTTGT-3' and 5'-ACAAGTCTCTGGAGCT GGACCAGAAGTTGTC-3'. For Gly73Trp: 5'-GGAGGCCCATGCCTG GAGGCATC-3' and 5'-GATGGCCTCCAGGATGGGCCTCC-3'. To mimic the truncated human VAMP2 Arg56* found in patients, the Arg56X (R56X) VAMP2-mOr2 construct was made by fusing the VAMP2 coding sequence for the first 55 amino acids to the N-terminus of mOr2 with the same linker as above, since introduction of a stop codon into the full-length VAMP2 cDNA would not allow expression of the downstream mOr2. All polymerase chain reaction (PCR)-generated VAMP2 sequences were verified by sequencing, then subcloned into the WT pCAGGS vector by *EcoRI* and *XhoI* using standard molecular biology methods. Synaptophysin-pHluorin (syp-pH) was made by inserting pHluorin flanked by a PCR-generated 5' linker (SGGTGGSGGTGGSGGTGGTGGSGGTGG) and 3' linker (SGGTGGSGGTGGSGGTGGSGGTGGSGGTGGSG) into an engineered Age1 site between amino acids 181T and 182G in the second luminal loop of rat synaptophysin (gift of R. Edwards, UCSF), generated by PCR-mediated mutagenesis, confirmed by sequencing, and subcloned into a pCAGGS vector.

To overexpress WT as well as variant VAMP2 in primary culture for electrophysiological experiments, lentiviral constructs carrying the corresponding cDNA sequences were subcloned into a pFUGW lentiviral vector using standard molecular biology techniques and verified by sequencing. Lentiviral particles were produced by transfecting HEK293T cells with the corresponding pFUGW transfer vector and three packaging plasmids (pVSVg, pMdlg/pPRE, and pRSV-Rev) using FuGENE 6 transfection reagent (Promega). Twenty-four hours after transfection, the HEK293T culture media was replaced by neuronal growth media. Lentiviral particles were released into the media over 48 h and harvested by low-speed centrifugation on the day of infection.

2.4 | Primary hippocampal culture, transfection, and lentiviral infection

For live-cell imaging experiments, hippocampi from embryonic day 19–20 rats of either sex were dissociated as previously described (Li,

Santos, Park, Dobry, & Voglmaier, 2017). Neurons were co-transfected with 0.8 μ g syp-pH and 0.2 μ g VAMP2-mOr2 in pCAGGS, using the Basic Neuron SCN Nucleofector Kit according to manufacturer's directions (Lonza). DNA amounts were optimized to produce relatively equal, moderate expression and punctate localization consistent with synaptic delivery (data not shown). All co-transfected VAMP2-mOr2 proteins co-localize with syp-pH in synaptic boutons (data not shown). Cells were maintained in Neurobasal media supplemented with 1% heat-inactivated fetal bovine serum, B27 (Gibco), 2 mM GlutaMax, 15 mM NaCl, and 10 μ g/ml MycoZap antibiotic (Lonza) and imaged at 14–19 days in vitro (DIV). 5-Fluoro-2'-deoxyuridine (10- μ M final concentration) was added at DIV3–5 as a mitotic inhibitor to control glial growth. This study with animals was conducted under the supervision of the UCSF Institutional Care and Use Committee.

For electrophysiology experiments, dissociated hippocampal cultures were prepared using postnatal 2–4 days old Sprague Dawley rats of either sex as previously described (Kavalali, Klingauf, & Tsien, 1999). On DIV4, neurons were infected by corresponding lentiviral particles per well in 24-well plates. Electrophysiology experiments were performed after DIV14, when synapses reach maturity, and overexpression of the target protein had plateaued. This study with animals was conducted under the supervision of the Vanderbilt University Medical Center Institutional Care and Use Committee.

2.5 | Live cell imaging and data analysis

Assessment of SV recycling by live-cell imaging was performed essentially as described previously (Li et al., 2017). Coverslips with transfected hippocampal neurons were mounted in a rapid switching, laminar-flow perfusion and stimulation chamber (Warner) on an inverted epifluorescence microscope (Nikon) and imaged at room temperature using a 60X oil objective (NA = 1.45). Cells were imaged in modified Tyrode's solution pH 7.4 (in mM: 119 NaCl, 10 HEPES-NaOH, 30 glucose, 2.5 KCl, 2 CaCl₂, 2 MgCl₂) containing 10 μ M each of the glutamate receptor inhibitors CNQX and CPP. Electrical stimulation to elicit APs was applied using an A310 Accupulser (WPI) at 5–100 Hz with 1 ms bipolar current pulses through platinum-iridium electrodes, to yield fields of 5–10 V/cm across the chamber. Cells were illuminated using a Xenon lamp (Sutter Instruments) with either a 470/40 nm excitation and a 525/50 nm emission filter for GFP, or a 545/25 nm excitation and 605/70 nm emission filter for mOr2 (Chroma). Images were acquired on a QuantEM CCD camera (Photometrics), exposing each fluorophore for 300 ms for images collected every 3 s. MetaMorph software was used to control data collection and to perform offline analysis (Molecular Devices). The total pool size was determined using Tyrode's solution with 50 mM NH₄Cl (NaCl reduced by 50 mM). To measure exocytosis alone, cultures were incubated in modified Tyrode's medium containing 0.5–1 μ M bafilomycin A for 30 s before imaging in the same medium. Neurons were incubated with 500 μ M DAP (Sigma) in media for 30 m before imaging in Tyrode's solution containing 200 μ M DAP.

MetaMorph software was used to quantify the average fluorescence of regions of interest (ROI) at synaptic sites at manually selected 4×4 pixel boxes placed over the center of boutons. The average fluorescence of three 4×4 pixel ROIs without cellular elements was subtracted as background. Baseline values from the first five frames (before stimulation) were averaged as initial fluorescence F_0 , and the dynamics of fluorescence intensity expressed as fractional change (ΔF) over initial fluorescence. For normalized measurements, the average pHluorin fluorescence over individual boutons was normalized to the total fluorescence visualized by application of modified Tyrode's solution containing 50 mM NH_4Cl to alkalize all synaptic compartments. Fluorescence measurements from 22 to 145 boutons per coverslip were averaged and the means from 7 to 12 coverslips from at least two independent cultures were averaged. The fraction of transporter that undergoes exocytosis (recycling pool [RP]) was measured as the fraction of the total pool that undergoes exocytosis in response to 10 Hz 90 s stimulation (Foss, Li, Santos, Edwards, & Voglmaier, 2013). The rate of exocytosis $[(\Delta F/F_0)/s]$ was estimated from a linear fit to the increase in pHluorin fluorescence during the initial 15 s of stimulation in the presence of bafilomycin.

2.6 | Electrophysiology and data analysis

Whole-cell patch-clamp recordings were performed on pyramidal cells using a CV203BU headstage, Axopatch 200B amplifier, Digidata 1320 digitizer, and Clampex 8.0 software (Molecular Devices). Recordings were filtered at 1 kHz and sampled at 100 s. For external bath solution, a modified Tyrode's solution containing the following was used: (in mM): 150 NaCl, 4 KCl, 2 MgCl_2 , 2 CaCl_2 , 10 glucose, 10 HEPES at pH 7.4. To isolate mEPSCs, 1 μM TTX, 50 μM PTX (picrotoxin), and 50 μM D-AP5 were added. To isolate evoked IPSCs, 50 μM D-AP5, and 10 μM CNQX was added. For evoked IPSC recordings, field stimulation was provided using a parallel bipolar electrode (FHC) immersed in the external bath solution, delivering 35 mA pulses. The 3–5 $\text{M}\Omega$ borosilicate glass patch pipettes were filled with the internal solution contained the following (in mM): 115 Cs-MeSO₃, 10 CsCl, 5 NaCl, 10 HEPES, 0.6 EGTA, 20 tetraethylammonium-Cl, 4 Mg-ATP, 0.3 Na_3GTP , and 10 QX-314 [N-(2,6-dimethylphenyl)carbamoylmethyl]-triethylammonium bromide] at pH 7.35 and 300 mOsm. For all recordings included for the analysis, membrane resistance was greater than 100 $\text{M}\Omega$, access resistance was less than 20 $\text{M}\Omega$ and time constant (τ) was less than 3 ms. mEPSC frequencies and amplitudes were analyzed using Mini Analysis software (Synaptosoft). Evoked IPSC peak amplitudes and cumulative charge transfer was analyzed by using Clampfit (Molecular Devices).

2.7 | Statistical analysis

Data are presented as mean \pm standard error of the mean. Graphpad Prism 8 was used for statistical analysis. The effects of variants were compared against WT VAMP2 by *t*-test. The mean difference was accepted as significant at $p < .05$.

3 | RESULTS

In this study, we describe five previously unreported, unrelated patients with novel *de novo* heterozygous VAMP2 pathogenic variants and their clinical characteristics (Table 1). Patients with these VAMP2 pathogenic variants were assessed by chart review and caretaker phone interviews. Parents provided written consent before participation. Common features include global developmental delay, autistic tendencies, and behavioral disturbances. The SNARE motif VAMP2 variants of Patients 1–3 were studied *in vitro*. Patients 4 and 5 were subsequently referred to our study.

3.1 | Case histories

Patient 1 (BRDP ID 2355-0) exhibited developmental delay and social impairments beginning in infancy. In adolescence she developed worsening behavioral problems, aggression, emotional lability, anxiety, hallucinations, and delusions. She was presumptively diagnosed with Hashimoto's encephalopathy and received empiric treatment with plasmapheresis, steroids and rituximab, with some degree of improvement in her mood and function with improved thyroid antibody titers, however, she still exhibited slowed psychomotor responsiveness and cognitive processing. Comprehensive work-up included CSF autoimmune encephalopathy panel (negative) and neurotransmitter metabolites (normal). MRI showed normal brain structure. Multiple extended EEGs had either moderate background slowing or were normal.

She came to UCSF as an adolescent after whole exome sequencing revealed a heterozygous *de novo* VAMP2 mutation (c.166C>T, p.Arg56X, where c. designates a location in the cDNA and p. designates a location in the predicted protein) predicting a premature truncation and haploinsufficiency from nonsense-mediated decay. Although not directly tested, this variant could also result in a dominant-negative effect. On initial evaluation, she had catatonia and was largely nonverbal with minimal motor activity. A nerve conduction study was undertaken to evaluate autonomic nerve function, where VAMP2 protein is expressed and hence activity is assayable. Sympathetic skin responses were very low amplitude, with relative preservation of response latencies, providing confirmation that VAMP2 haploinsufficiency caused symptoms.

Patient 2 (BDP 2362-0) is a 39-year-old male with cognitive impairment, autism spectrum disorder (ASD), epilepsy, and retinitis pigmentosa. Parents noticed nystagmus during infancy, and he was evaluated at age 3 years for developmental delay. Whole exome testing revealed a VAMP2 variant (heterozygous *de novo* c.217G>T, p.Gly73Trp). This is predicted to be a missense mutation causing a dominant-negative effect. He independently performs some activities of daily living, such as showering, toileting, and dressing, and participates in a sheltered workshop program. He uses basic appliances and repairs simple things. He speaks in complete sentences and converses, but he displays obsessive-compulsive tendencies, restricted interests, and echolalia. Progressively worsening ataxia and

TABLE 1 Clinical features of patients with *de novo* VAMP2 mutations

Patient number	1	2	3	4	5
Variant	Heterozygous <i>de novo</i> c.166C>T, p.Arg56X	Heterozygous <i>de novo</i> c.217G>T, p.Gly73Trp	Heterozygous <i>de novo</i> c.167G>T, p.Arg56Leu	Heterozygous <i>de novo</i> c.337_341 deletion TACTT p.Tyr113Gln frameshift, creating stop codon 12	Heterozygous <i>de novo</i> c.1A>G, p. Met1?
Predicted change	Premature truncation, causing haploinsufficiency	Missense mutation, causing dominant-negative effect	Missense mutation, causing dominant-negative effect	Frameshift deletion creating a premature stop codon, causing haploinsufficiency	Elimination of initiator methionine could result in no protein, truncated protein, most likely haploinsufficiency
Age	20	39	5	6	5
Gender	F	M	M	M	M
Age of presentation	Infancy	3 Years	Unknown	18 Months	1 Year
Clinical seizures	No	Generalized convulsions	Infantile spasms, focal, and tonic seizures	No	No
EEG	Reduced organization or normal	Excessive generalized slowing	Burst suppression, hypersarrhythmia	Not done	Not done
Visual deficits	Visual acuity deficits	Retinitis pigmentosa	CVI	None	Hypermetropia and astigmatism
Speech impairment	No	Echolalia	Nonverbal	Speech delay	Speech delay
Movement disorder	Catatonia	Nystagmus, progressive ataxia, tremor	No	No	No
Dysautonomia	Autonomic and small fiber neuropathy	Not tested	Frequent unexplained fevers, no formal testing	Not tested	Not tested
Psychiatric features	Hallucinations, delusions, anxiety, depression	Obsessive-compulsive tendencies	Unable to assess	Hyperactivity, impulsivity	Hyperactivity, impulsivity
Behavioral disturbances	Aggressive outbursts, self-injurious behavior	No	Unable to assess due to severe ID	Aggressive outbursts, self-injurious behavior	Aggressive outbursts
Autistic features	Yes	Yes	Unable to assess due to severe ID	Yes	No
Brain imaging	Normal	Periventricular FLAIR hyperintensities	Hypoplastic corpus callosum	Not done	Normal
Ancillary studies	EMG with reduced sympathetic skin responses	None	None	None	None

(Continues)

TABLE 1 (Continued)

Patient number	1	2	3	4	5
Global DD	Yes	Yes	Yes	Yes	Yes
Dysmorphisms	Mild hypertelorism	None	Growth restricted	Short stature	None
Level of independence	Performs all ADLs	Independent in most ADLs	Completely dependent	Age appropriate	Age appropriate

Note: Variants were reported through whole exome testing by GeneDx, where c. designates a location in the cDNA and p. designates a location in the predicted protein. Abbreviations: ADL, activities of daily living; DD, developmental delay; EEG, electroencephalography; EMG, electromyography; ID, intellectual disability.

tremor impair his ability to walk and write. He developed epilepsy at 3 years of age, described as full-body convulsions, which has been relatively well-controlled on oxcarbazepine and more recently lamotrigine. Parents describe him as mellow, helpful, and cooperative; he does not have behavioral aggression or hallucinations.

Patient 3 was identified by a clinical laboratory by whole exome testing. He carries a *de novo* VAMP2 variant (heterozygous *de novo* c.167G>T, p.Arg56Leu) predicted to cause an amino acid missense mutation predicted to result in a dominant-negative effect. He is a 6-year-old child with refractory infantile spasms and global developmental delay. EEG showed burst-suppression and hypsarrhythmia. MRI of the brain demonstrated a mildly hypoplastic corpus callosum. Severe intellectual disability confounds any behavioral or autistic features that might be present.

Patient 4 was born at term without complications after an uneventful pregnancy. At 18 months of age, parents noticed issues with speech and gross motor skills. He was evaluated through their regional center and began receiving services (speech, occupational, and physical therapies). Whole exome sequencing at 4 years of age revealed a variation in VAMP2 (heterozygous *de novo* c.337_341 deletion TACTT p.Tyr113Gln frameshift, predicted to create a stop codon 12 [p.Tyr113GlnfsX12]), and resulting haploinsufficiency. Later he was diagnosed with ASD and attention deficit hyperactivity disorder (ADHD). He also carries a maternally inherited deletion of unclear significance (15q13.3 between D-CHRNA7 to BP5 arr[GRCh37] 15q13.3 [32024132_32509926; size: 486 Kb]). The patient's mother is cognitively normal. Reports show incomplete penetrance of this deletion, ranging from mildly affected to normal individuals (Shinawi et al., 2009). While an additive contribution of this deletion to the VAMP2 phenotype in this patient cannot be excluded, it remains uncertain given that the patient's mother is phenotypically normal. Currently 6 years old, he is making developmental progress in prekindergarten with services. He can speak in short sentences and can repeat phrases; however, does not know primary colors or ABCs. For fine motor skills, he can color. He walks independently but is clumsy and falls frequently. He exhibits aggressive outbursts and self-injurious behavior. He is hyperactive and impulsive, for which he takes stimulant medications. He does not have a history of seizures or movement disorders.

Patient 5 was born at term, and the pregnancy was complicated by polyhydramnios and decreased fetal movements. Parents first noticed developmental differences at 1 year of age, mainly involving speech but eventually including low muscle tone and frequent falls. At 1 year of age, he spoke no words. Audiometry showed a mild hearing loss, likely due to frequent ear infections, which resolved with tympanostomy tubes. His family noticed frequent falls (upwards of 30 falls per day), trouble climbing stairs, and difficulty transitioning from different positions. With therapies (speech, occupational, and physical), he saw slow improvement in these domains; however, his mother estimates he continues functioning several years behind expected milestones. Currently, 5 years old, he speaks in five-word sentences but has trouble understanding multistep commands and is slow to process verbal information. He can run, walk slowly upstairs, and scribble with a coarse grasp. He continues to fall several times per day

and has trouble with fine coordination, most noticeable when attempting to feed himself with utensils. Parents say he is very cautious and has trouble with depth perception. His mother describes him as sweet and soft-spoken but does have aggressive outbursts when overwhelmed or overstimulated. Whole exome sequencing was performed and revealed a heterozygous *de novo* c.1A>G, p. Met1? VAMP2 mutation. This change is thought to cause the elimination of the initiator methionine, which could result in no protein formation, or a truncated protein with a different initiator amino acid. For additional workup, brain MRI was obtained and normal. He received an autism evaluation at age 3, and did not meet the criteria for autism, but displayed ADHD tendencies. There have been no concerns for seizures. The patient has an older brother with ADHD and dyslexia and a healthy younger sister. There is a first cousin with autism.

3.2 | VAMP2 variants decrease the rate and extent of SV exocytosis

To investigate potential dominant-negative effects of disease-associated VAMP2 SNARE motif variants on SV protein trafficking in cellular models, we used live-cell imaging of an optical reporter of SV recycling, syp-pH. Syp-pH is a fusion of the pH-sensitive green fluorescent protein pHluorin to a luminal domain of synaptophysin, an integral membrane protein that associates with VAMP2 on SVs (Figure 1b; Calakos & Scheller, 1994; Li et al., 2017). Transfected into hippocampal neurons in culture, syp-pH fluorescence is quenched at the acidic pH of SVs. Exocytosis induced by electrical stimulation increases syp-pH fluorescence as quenching is relieved upon exposure of the SV lumen to the higher external pH during fusion. After stimulation, fluorescence decreases due to internalization of the reporter and reacidification of SVs upon endocytosis (Figure 1a,b). Since VAMP2 mediates vesicle fusion, we first measured syp-pH exocytosis in neurons cotransfected with WT or variant VAMP2-mOr2 in the presence of the vacuolar H⁺-ATPase inhibitor bafilomycin. Bafilomycin blocks reacidification of SVs that have taken up the drug after exocytosis, eliminating fluorescence changes due to endocytosis. Compared with WT, cotransfection of Gly73Trp (G73W, Patient 2) or Arg56Leu (R56L, Patient 3) VAMP2 variants results in a slower rate of fluorescence increase, corresponding to slower exocytosis, in response to 900 APs, which releases the RP of SVs (Figure 1c,d). The extent of exocytosis, reflecting the number of SVs released from the RP, is also decreased for Gly73Trp (G73W, Patient 2) and Arg56Leu (R56L, Patient 3) compared to WT. An effect of the Arg56X mutation (R56X, Patient 1) was not detected, perhaps because the truncation lacks the transmembrane domain responsible for synaptophysin interaction and membrane localization (Edelmann, Hanson, Chapman, & Jahn, 1995).

3.3 | K⁺ efflux blocker DAP increases SV exocytosis

To test whether prolonging the AP by blocking K⁺ outflow affects exocytosis, we incubated neurons with the K⁺ channel inhibitor DAP.

Compared with control, DAP treatment of neurons cotransfected with WT VAMP2 significantly increases the rate and extent of syp-pH exocytosis (Figure 1c,d). DAP also significantly increases the rate and extent of syp-pH exocytosis in neurons cotransfected with Arg56X (R56X, Patient 1), Gly73Trp (G73W, Patient 2), or Arg56Leu (R56L, Patient 3) to a level similar to WT + DAP.

Changes in exocytosis could also result from differences in endocytosis or release site clearance. Since several residues in the SNARE motif of VAMP2 have been implicated in SV endocytosis (Grote & Kelly, 1996), we also tested the effects of the VAMP2 variants on endocytosis of syp-pH in the absence of bafilomycin. The poststimulus fluorescence decay of syp-pH, representing endocytosis, is not significantly altered by any of the VAMP2 variants compared with WT (Figure 2). The addition of DAP does not significantly affect the endocytosis rate but does increase peak fluorescence levels, consistent with the demonstrated effects of DAP on exocytosis. Data quantifications are reported in Table S1.

3.4 | Effects of VAMP2 variants and DAP on AP evoked release

To investigate effects of VAMP2 variants on AP triggered evoked neurotransmitter release, whole cell patch-clamp electrophysiology was used to record inhibitory currents from primary hippocampal neurons expressing WT VAMP2 or VAMP2 variants. We recorded inhibitory postsynaptic currents to avoid the high-frequency spontaneous AP firing and recurrent excitation that contaminates excitatory recordings (Maximov, Shin, Liu, & Sudhof, 2007). In response to a single AP, Gly73Trp (G73W, Patient 2) and Arg56Leu (R56L, Patient 3) VAMP2 variants respond less than WT, measured by synaptic charge transfer (Figure 3a). In this assay, Arg56X (R56X, Patient 1) responds similarly to WT. No variants changed miniature current amplitudes, suggesting an effect on the presynaptic release machinery without changing the number of postsynaptic receptors (data not shown).

When multiple APs are applied at short time intervals causing SV depletion, successive postsynaptic responses decrease in amplitude. In addition, higher release probability is associated with more robust synaptic depression, since the initial stimulation causes release of more SVs, leaving only a few to be released in response to the following stimulations. As expected, WT VAMP2 depressed to $22 \pm 3.57\%$ of the first response in response to the 10th AP at 10 Hz (Figure 3b). Consistent with live imaging results, Gly73Trp (G73W, Patient 2) and Arg56Leu (R56L, Patient 3) depress less than WT, suggesting that the release probability in the presence of these variants is lower compared to WT. Arg56X (R56X, Patient 1) does not affect synaptic depression. DAP causes release to become more asynchronous, thus increasing overall synaptic charge transfer (Figure 3a). This increase in charge transfer is also associated with higher release probability, as suggested by more robust synaptic depression (Figure 3b).

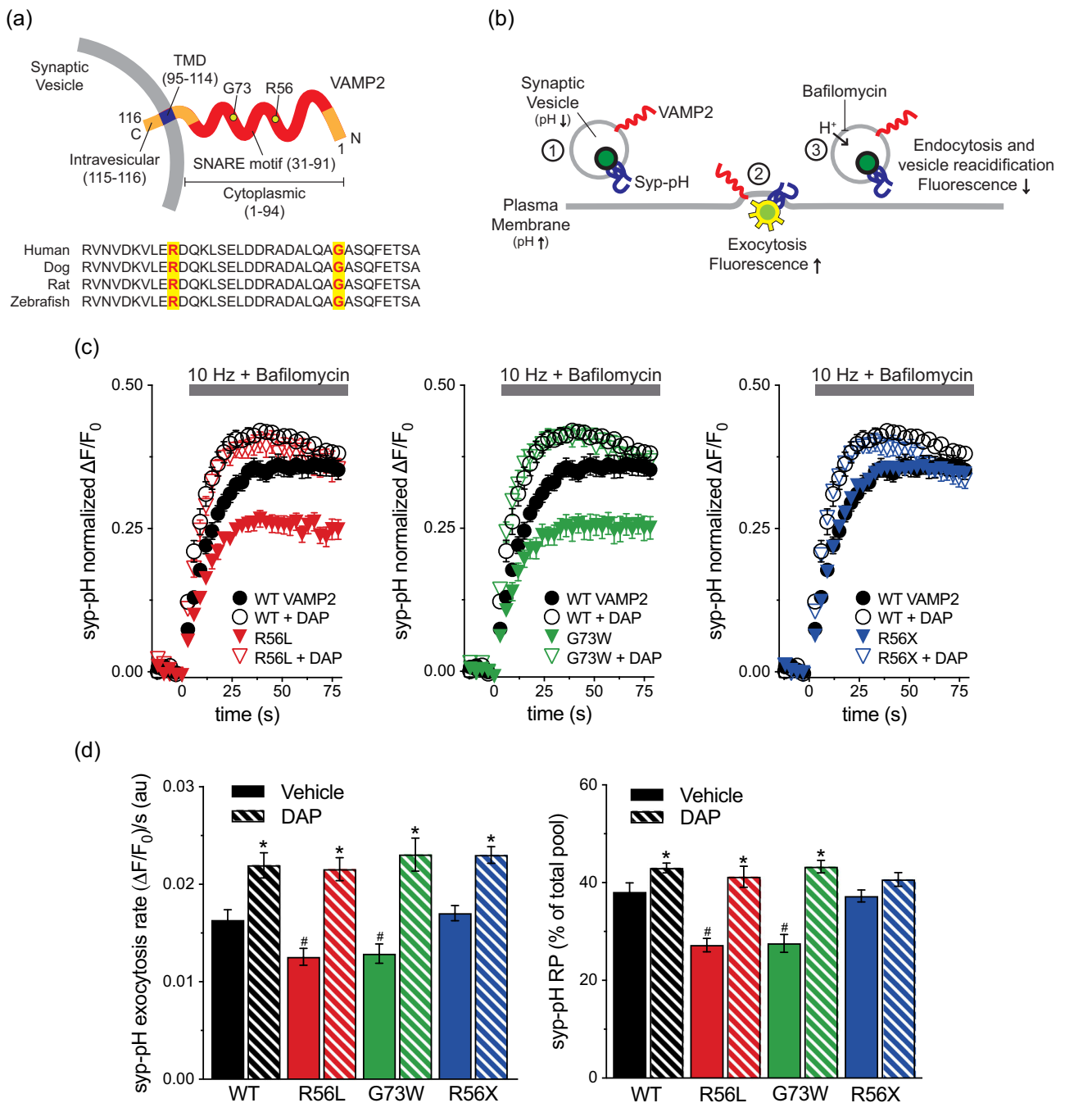


FIGURE 1 K⁺channel blocker rescue of vesicle-associated membrane protein 2 (VAMP2) mutation-induced exocytosis defects in vitro. (a) Schematic of human VAMP2 depicts the C-terminal transmembrane domain (TMD), cytoplasmic soluble N-ethylmaleimide-sensitive factor attachment protein receptor (SNARE) motif, and variant amino acids. The alignment shows the sequence conservation of the SNARE motif across species. (b) Schematic of live-cell imaging of synaptic vesicle (SV) recycling. (1) Synaptophysin-pHluorin (syp-pH) fluorescence is quenched at low SV pH. (2) Electrical stimulation to elicit exocytosis relieves fluorescence quenching upon exposure of the luminal syp-pH to higher external pH. (3) After stimulation, syp-pH fluorescence decreases upon endocytosis and reacidification of SVs by the vacuolar H⁺-ATPase. The vacuolar H⁺-ATPase inhibitor bafilomycin in the external media blocks reacidification of SVs that have taken up the drug, eliminating fluorescence changes due to endocytosis. (c) Time course of exocytosis in response to 10 Hz stimulation in bafilomycin, in neurons cotransfected with the indicated VAMP2-mOr2 constructs, with vehicle or 3,4-diaminopyridine (DAP). (d) Quantification of the rate and extent of exocytosis from the recycling SV pool (RP), as a percent of the total pool. Arg56Leu (p.R56L) and Gly73Trp (p.G73W) variants decrease exocytosis rate and extent compared with wild-type (WT; #*p* < .05 for each). Arg56X (p.R56X) truncation is similar to WT. DAP increases the extent of exocytosis with WT, p.R56L, and p.G73 variants, compared with control (**p* < .05). The exocytosis rate is increased with all VAMP2 constructs (**p* < .01 each). Data are means \pm SEM of the change in fluorescence (ΔF) normalized to initial fluorescence (F_0) over at least 23 boutons per coverslip from 9 to 12 coverslips from at least three independent cultures. Significance determined by *t*-tests

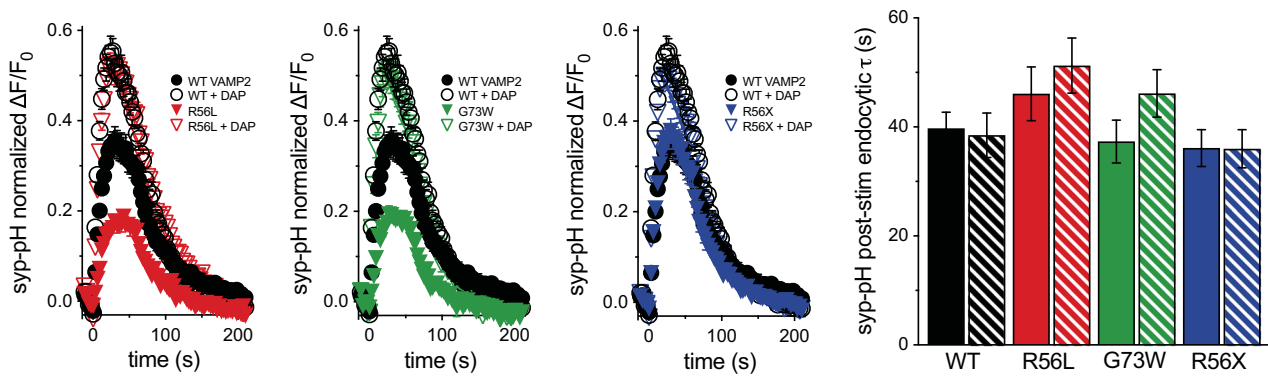


FIGURE 2 No effect of 3,4-diaminopyridine (DAP) on endocytosis. In the absence of bafilomycin, there are no significant differences in poststimulus endocytosis rates between wild-type (WT) vesicle-associated membrane protein 2 (VAMP2) and any of the variants, or with DAP treatment. Data are means \pm SEM of the change in fluorescence (ΔF) normalized to initial fluorescence (F_0) over at least 22 boutons per coverslip from 7 to 9 coverslips and at least two independent cultures. Significance determined by *t*-tests

3.5 | Clinical course

Extrapolating from *in vitro* studies, we hypothesized 4-AP could improve clinical outcomes in patients harboring VAMP2 pathogenic variants. After minimal efficacy with prior treatments using plasmapheresis, steroids and rituximab, Patient 1 was begun on an off-label treatment with 4-AP (Ampyra; Acorda Therapeutics) beginning March 2018 when she was 18 years of age, starting at low-dose (2.5 mg TID) and increasing over several months to maximal clinical efficacy and tolerability. Benefits were measured by qualitative assessments (subjective parental reports) and quantitatively (neuropsychological testing). Tolerability was assessed by parental report of worsening anxiety or insomnia. Within 2 months, she experienced dramatic improvement, most notably in social interaction. She seemed to “awaken.” She was calmer, attentive, socially engaging, with increased verbal and motor output. During a period of accidental half dosing, she returned to the pretreatment state; symptoms improved with correct dosing. In April 2019, she developed tolerance to 4-AP, so it was increased to 7.5 mg AM and 5 mg PM extended release (XR). She responded with additional improvements in sleep and mood.

After optimal dosing of 5 mg TID XR, she completed a neuropsychological evaluation in May 2019. Compared with prior evaluations in 2017, the speed of information processing and verbal memory recall improved by 133%. Neuropsychological testing pre- and posttreatment were compared by converting scaled scores to Z-scores. Other cognitive functions appeared stable (Table 2). Parents reported improvement in emotional and behavioral regulation; she was less labile and more interactive. A worsening of preexisting anxiety accompanied cognitive improvements, perhaps from increased insight into her limitations. This anxiety was responsive to subsequent introduction of low dose (10 mg TID) propranolol.

4 | DISCUSSION

In this study, we identified five individuals with novel *de novo* heterozygous pathogenic variants in VAMP2, a key SV protein.

They presented with global developmental delay, autistic features, behavioral disturbances, and a higher propensity to develop epilepsy. Furthermore, we showed that the missense variants of VAMP2, Gly73Trp (Patient 2) and Arg56Leu (Patient 3), associated with a more severe phenotype with epilepsy *in vivo*, exert a dominant-negative effect on AP-triggered SV fusion and neurotransmitter release *in vitro*. Consistent with these results, the recent report by Salpietro et al. (2019) suggested that an independently identified disease-associated VAMP2 variant in close proximity to the Gly73Trp (Patient 2) variant described here, Ser75Pro, impairs vesicle fusion of reconstituted membranes *in vitro* in a dominant-negative manner. In contrast, the nonsense variant (Arg56X, Patient 1) does not cause dominant-negative effects, suggesting that haploinsufficiency underlies the disease mechanism for the R56X variant patient, who presented with a milder phenotype without epilepsy. Since both missense and nonsense variants are associated with impaired AP-triggered neurotransmitter release, we hypothesized that prolonging local Ca^{2+} availability by inhibiting K^+ channels with 4-AP could increase the probability of release, thus restoring synaptic transmission (Storm, 1987; Wheeler, Randall, & Tsien, 1996). As expected, we showed that treatment with the 4-AP analog DAP corrects the *in vitro* deficits associated with the VAMP2 variants. In particular, in prolonging the period in which local Ca^{2+} concentration is high enough to trigger neurotransmitter release, DAP switched the mode of release from fast-synchronous to asynchronous. This, in turn, increases overall synaptic charge transfer, thus rescuing the deficits in neurotransmitter release. Given that DAP functions through prolonging AP duration and increasing release probability, the effect of DAP may vary in presynaptic terminals releasing different neurotransmitters. For example, GABAergic terminals, which comprise the main inhibitory system of CNS, typically have a higher probability of release than glutamatergic terminals, the main excitatory system. Disturbances of excitatory–inhibitory balance in neuronal circuits may underlie certain neuropsychiatric disorders and enhancement of inhibitory neurotransmission has been shown

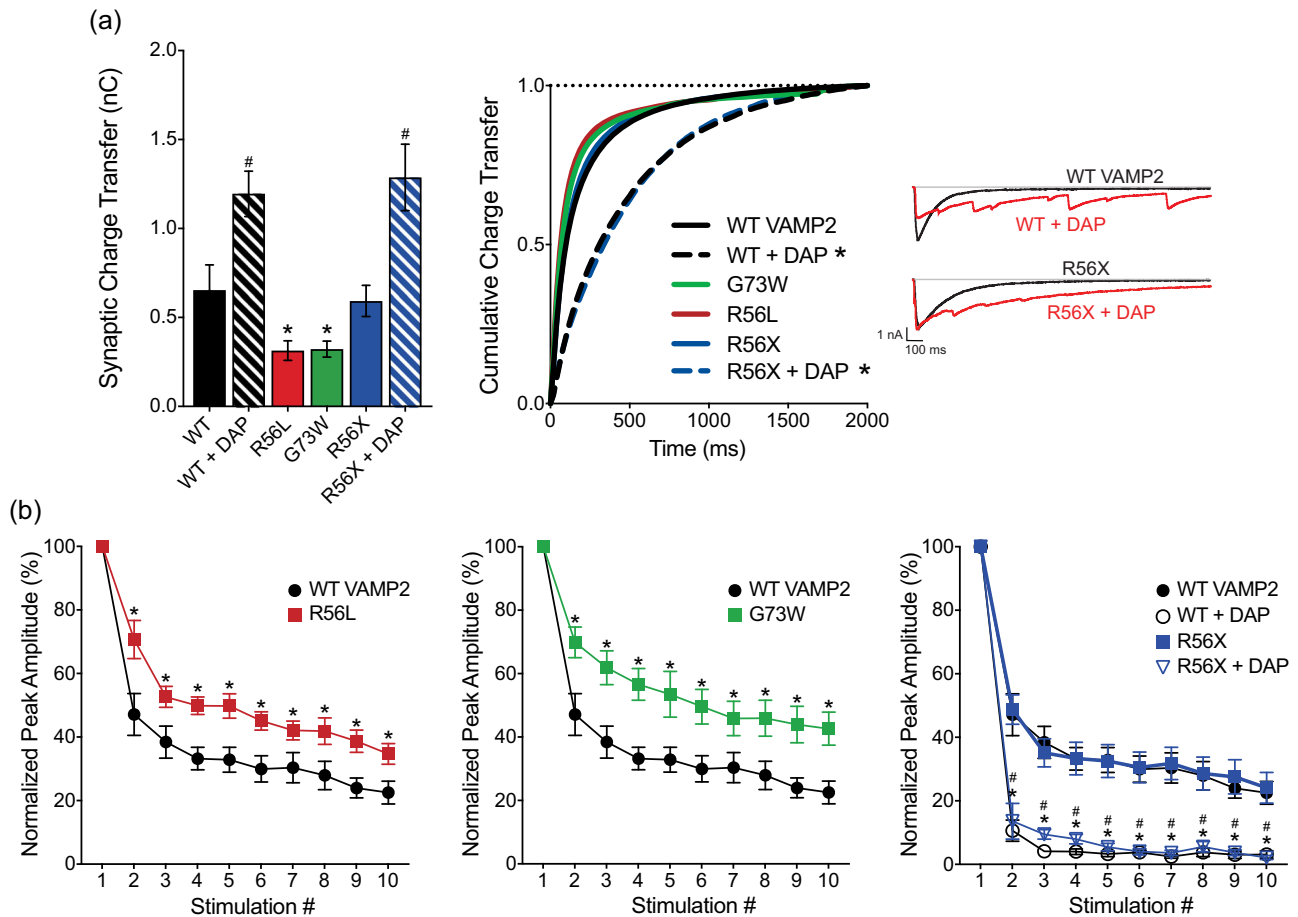


FIGURE 3 Effects of vesicle-associated membrane protein 2 (VAMP2) variants and 3,4-diaminopyridine (DAP) on evoked release. (a) p.R56L and p.G73W variants decrease the overall synaptic charge transfer, measured as the area under the curve of an evoked inhibitory postsynaptic current (eIPSC). DAP treatments increase synaptic charge transfer (wild-type [WT]: 0.655 ± 0.141 nC, WT + DAP: 1.195 ± 0.128 nC, p.R56L: 0.315 ± 0.055 nC, p.G73W: 0.323 ± 0.045 nC, p.R56X: 0.593 ± 0.088 nC, p.R56X + DAP: 1.287 ± 0.187 nC, $*p < .05$ for WT vs. p.R56L and WT vs. p.G73W, $^{\#}p < .05$ for WT vs. WT + DAP and p.R56X vs. p.R56X + DAP, two-tailed t-test). Variants do not change the synchronicity of the release ($*p > .05$ for WT vs. p.R56L, p.G73W and p.R56X, Kolmogorov–Smirnov test), but corresponding 3,4-DAP treatments result in more asynchronous release ($*p < .001$ for both WT vs. WT + DAP and p.R56X vs. p.R56X + DAP, Kolmogorov–Smirnov test). (b) Normalized peak amplitudes of eIPSCs in response to 10 consecutive stimulations at 10 Hz. p.G73W and p.R56L variants cause less depression after initial stimulation compared to WT VAMP2 ($*p < .05$ for WT VAMP2 vs. p.G73W and WT VAMP2 vs. p.R56L, multiple t-tests for each stimulation). Although p.R56X responds similarly as WT, corresponding DAP treatments cause more robust depression in response to stimulation ($p < .05$ for $^{\#}$ WT vs. WT + DAP and $^{\#}$ p.R56X vs. p.R56X+DAP, multiple t-tests for each stimulation)

to ameliorate some behavioral deficits in mouse models of autism (Sohal & Rubenstein, 2019).

Extrapolating from in vitro studies, we started 4-AP (Ampyra) treatment for Patient 1, the Arg56X affected individual, in 2018. She responded dramatically, confirming that in vitro studies successfully predicted clinical response. With treatment for the last 2 years, Patient 1 shows remarkable improvement in cognitive processing speed and verbal memory recall. Treatment drastically improved the quality of life for our patient and her family given her enhanced ability to interact and decreased emotional lability. In this study, we demonstrate that augmentation of neurotransmitter release by aminopyridines can be a viable treatment option for VAMP2 associated disorders with impaired neurotransmitter release. Most importantly, we showed the first

evidence of clinical improvement upon 4-AP treatment in a patient harboring a nonsense variant of VAMP2. 4-AP could treat other patients with VAMP2 or other SNARE protein mutations. Our results are in agreement with recent in vitro studies showing that DAP also can overcome release deficits associated with disease-causing synaptotagmin-1 variants (Bradberry et al., 2020). Taken together, these observations confirm and expand our hypothesis that augmentation of release by DAP or 4-AP would be a viable treatment option for other SNAREopathies as well (Baker et al., 2018; Harper, Mancini, van Slegtenhorst, & Cousin, 2017; Salpietro et al., 2017; Verhage & Sorensen, 2020). This approach could be tested in vitro before clinical implementation. 4-AP should be used cautiously in patients with epilepsy given the risk of lowering the seizure threshold, which can limit its broad-based

TABLE 2 Comparison of neuropsychological testing scores for patient 1

	2017	2019	2017	2019	Change in Z-score
WRAML-2	No. of correct/recalled		Scaled score		
Sentence memory	14	16	1	3	0.67
Story memory (Immediate)	5	12	1	4	1.00
Story memory delay recall	0	11	1	4	1.00
Verbal learning (immediate)	15	20	2	3	0.33
Verbal learning delay recall	7	10	7	9	0.67
Design memory (immediate)	13	14	1	2	0.33
Design memory delayed recognition	25	21	5	1	-1.33
Picture memory (immediate)	18	23	4	6	0.67
Picture memory delayed recognition	30	29	6	5	-0.33
D-KEFS trail making test	Time to completion		Scaled score		
Visual scanning	31	34	6	4	-0.67
Number sequencing	106	53	1	4	1.00
Letter sequencing	53	40	3	7	1.33
Number-letter switching	203	136	1	2	0.33
Motor speed	61	43	3	7	1.33
D-KEFS verbal fluency	No. of correct within time limit		Scaled score		
Letter fluency	6	7	1	1	0.00
Category fluency	8	12	1	1	0.00
Category switching total	7	6	3	2	-0.33
Category Switching Accuracy	5	4	4	3	-0.33
Golden stroop	No. of correct within time limit		T score		
Word score	52	60	18	25	0.70
Color score	35	41	16	22	0.60
Color-word score	23	20	33	31	-0.20
Interference score	3	-4	53	46	-0.70

Note: Comparison between neuropsychological evaluations from May 2019 (UCSF) while on optimal dosing of 4-AP to prior evaluations in 2017 (Sutter) before starting treatment. Results show speed of information processing and verbal memory recall improved by 133%. Other cognitive functions appeared stable. UCSF testers were blinded to prior results from 2017 but not to treatment with 4-AP.

Abbreviations: 4-AP, 4-aminopyridine; UCSF, University of California, San Francisco.

utility. Two of the patients with dominant, missense SNARE motif mutations had epilepsy (Patient 2, Gly73Trp and Patient 3, Arg56Leu) whereas two patients with heterozygous loss of function mutations (Patient 1, Arg56X and Patient 4, Tyr113GlnfsX12) did not have seizures, but did share the same range of behavioral deficits. Consistent with a prior study of five patients by Salpietro et al., the patients in our cohort also display global developmental delay, autistic features, and behavioral disturbances. Additional patients will better and more fully characterize the VAMP2 phenotype.

ACKNOWLEDGMENTS

This study was supported by the National Institutes of Health (MH083691 to Susan M. Voglmaier; MH066198 to Ege T. Kavalali; NS058721 to Elliott H. Sherr) and the University of California, San Francisco.

CONFLICT OF INTERESTS

The authors declare that there are no conflict of interests.

AUTHOR CONTRIBUTORS

Susan M. Voglmaier, Elliott H. Sherr, and Ege T. Kavalali conceived, designed, and supervised the study. All authors were involved in the acquisition, analysis, and interpretation of data. Roxanne L. Simmons, Susan M. Voglmaier, Elliott H. Sherr, Ege T. Kavalali, Baris Alten, and Haiyan Li drafted and critically revised the manuscript for important intellectual content. Susan M. Voglmaier and Elliott H. Sherr are responsible for the overall content of the manuscript.

DATA AVAILABILITY STATEMENT

The data that support the findings of this study are available on request from the corresponding author. The data are not publicly available due to privacy or ethical restrictions.

WEB RESOURCES

GeneDx

<http://www.genedx.com>

ClinVar

<http://www.ncbi.nlm.nih.gov/clinvar/>

Poly-Phen2

<http://genetics.bwh.harvard.edu/pph2/>

GnomAD

<http://gnomad.broadinstitute.org>

ACCESSION NUMBERS FROM CLINVAR FOR VAMP2

VARIANTS

Patient 1: SUB7621453; c.166C>T, p.Arg56X

<http://www.ncbi.nlm.nih.gov/clinvar/variation/929460/>

Patient 2: SUB7630353; c.217G>T, p.Gly73Trp

<http://www.ncbi.nlm.nih.gov/clinvar/variation/929461/>

Patient 3: SUB7630360; c.167G>T; p.Arg56Leu

<http://www.ncbi.nlm.nih.gov/clinvar/variation/929463/>

Patient 4: SUB7630356; c.337_341delTACTT, p.Tyr113GlnfsX12

<http://www.ncbi.nlm.nih.gov/clinvar/variation/929464/>

Patient 5: SUB7630357; c.1A>G, p. Met1?

<http://www.ncbi.nlm.nih.gov/clinvar/variation/929462/>

ORCID

Marwan Shinawi  <http://orcid.org/0000-0003-1329-4100>Susan M. Voglmaier  <http://orcid.org/0000-0002-1211-8108>

REFERENCES

- Baker, K., Gordon, S. L., Melland, H., Bumbak, F., Scott, D. J., Jiang, T. J., ... Raymond, F. L. (2018). SYT1-associated neurodevelopmental disorder: A case series. *Brain*, 141(9), 2576–2591. <https://doi.org/10.1093/brain/awy209>
- Bradberry, M. M., Courtney, N. A., Dominguez, M. J., Lofquist, S. M., Knox, A. T., Sutton, R. B., & Chapman, E. R. (2020). Molecular basis for synaptotagmin-1-associated neurodevelopmental disorder. *Neuron*, 107(1), 57–64.e7. <https://doi.org/10.1016/j.neuron.2020.04.003>
- Calakos, N., & Scheller, R. H. (1994). Vesicle-associated membrane protein and synaptophysin are associated on the synaptic vesicle. *Journal of Biological Chemistry*, 269(40), 24534–24537.
- Claassen, J., Teufel, J., Kalla, R., Spiegel, R., & Strupp, M. (2013). Effects of dalfampridine on attacks in patients with episodic ataxia type 2: An observational study. *Journal of Neurology*, 260(2), 668–669. <https://doi.org/10.1007/s00415-012-6764-3>
- Deak, F., Schoch, S., Liu, X., Sudhof, T. C., & Kavalali, E. T. (2004). Synaptobrevin is essential for fast synaptic-vesicle endocytosis. *Nature Cell Biology*, 6(11), 1102–1108.
- Edelmann, L., Hanson, P. I., Chapman, E. R., & Jahn, R. (1995). Synaptobrevin binding to synaptophysin: A potential mechanism for controlling the exocytotic fusion machine. *EMBO Journal*, 14(2), 224–231.
- Fasshauer, D., Eliason, W. K., Brunger, A. T., & Jahn, R. (1998). Identification of a minimal core of the synaptic SNARE complex sufficient for reversible assembly and disassembly. *Biochemistry*, 37(29), 10354–10362.
- Foss, S. M., Li, H., Santos, M. S., Edwards, R. H., & Voglmaier, S. M. (2013). Multiple dileucine-like motifs direct VGLUT1 trafficking. *The Journal of Neuroscience*, 33(26), 10647–10660. <https://doi.org/10.1523/JNEUROSCI.5662-12.2013>
- Grote, E., & Kelly, R. B. (1996). Endocytosis of VAMP is facilitated by a synaptic vesicle targeting signal. *Journal of Cell Biology*, 132, 537–547.
- Harper, C. B., Mancini, G. M. S., van Slegtenhorst, M., & Cousin, M. A. (2017). Altered synaptobrevin-II trafficking in neurons expressing a synaptophysin mutation associated with a severe neurodevelopmental disorder. *Neurobiology of Disease*, 108, 298–306. <https://doi.org/10.1016/j.nbd.2017.08.021>
- Jahn, R., & Scheller, R. H. (2006). SNAREs—Engines for membrane fusion. *Nature Reviews Molecular Cell Biology*, 7(9), 631–643. <https://doi.org/10.1038/nrm2002>
- Kavalali, E. T., Klingauf, J., & Tsien, R. W. (1999). Activity-dependent regulation of synaptic clustering in a hippocampal culture system. *Proceedings of the National Academy of Sciences of the United States of America*, 96(22), 12893–12900. <https://doi.org/10.1073/pnas.96.22.12893>
- Koo, S. J., Markovic, S., Puchkov, D., Mahrenholz, C. C., Beceren-Braun, F., Maritzen, T., ... Haucke, V. (2011). SNARE motif-mediated sorting of synaptobrevin by the endocytic adaptors clathrin assembly lymphoid myeloid leukemia (CALM) and AP180 at synapses. *Proceedings of the National Academy of Sciences of the United States of America*, 108(33), 13540–13545. <https://doi.org/10.1073/pnas.1107067108>
- Li, H., Santos, M. S., Park, C. K., Dobry, Y., & Voglmaier, S. M. (2017). VGLUT2 trafficking is differentially regulated by adaptor proteins AP-1 and AP-3. *Frontiers in Cellular Neuroscience*, 11, 324. <https://doi.org/10.3389/fncel.2017.00324>
- Maximov, A., Shin, O. H., Liu, X., & Sudhof, T. C. (2007). Synaptotagmin-12, a synaptic vesicle phosphoprotein that modulates spontaneous neurotransmitter release. *Journal of Cell Biology*, 176(1), 113–124.
- Mohrmann, R., & Sorensen, J. B. (2012). SNARE requirements en route to exocytosis: From many to few. *Journal of Molecular Neuroscience*, 48(2), 387–394. <https://doi.org/10.1007/s12031-012-9744-2>
- Monteggia, L. M., Lin, P. Y., Adachi, M., & Kavalali, E. T. (2018). Behavioral analysis of SNAP-25 and synaptobrevin-2 haploinsufficiency in mice. *Neuroscience*, 420, 129–135. <https://doi.org/10.1016/j.neuroscience.2018.08.014>
- Palace, J., Wiles, C. M., & Newsom-Davis, J. (1991). 3,4-Diaminopyridine in the treatment of congenital (hereditary) myasthenia. *Journal of Neurology, Neurosurgery and Psychiatry*, 54(12), 1069–1072. <https://doi.org/10.1136/jnnp.54.12.1069>
- Salpietro, V., Lin, W., Delle Vedove, A., Storbeck, M., Liu, Y., Efthymiou, S., ... Houlden, H. (2017). Homozygous mutations in VAMP1 cause a presynaptic congenital myasthenic syndrome. *Annals of Neurology*, 81(4), 597–603. <https://doi.org/10.1002/ana.24905>
- Salpietro, V., Malintan, N. T., Llano-Rivas, I., Spaeth, C. G., Efthymiou, S., Striano, P., ... Houlden, H. (2019). Mutations in the neuronal vesicular SNARE VAMP2 affect synaptic membrane fusion and impair human neurodevelopment. *American Journal of Human Genetics*, 104(4), 721–730. <https://doi.org/10.1016/j.ajhg.2019.02.016>
- Shaner, N. C., Lin, M. Z., McKeown, M. R., Steinbach, P. A., Hazelwood, K. L., Davidson, M. W., & Tsien, R. Y. (2008). Improving the photostability of bright monomeric orange and red fluorescent proteins. *Nature Methods*, 5(6), 545–551.
- Shinawi, M., Schaaf, C. P., Bhatt, S. S., Xia, Z., Patel, A., Cheung, S. W., ... Stankiewicz, P. (2009). A small recurrent deletion within 15q13.3 is associated with a range of neurodevelopmental phenotypes. *Nature Genetics*, 41(12), 1269–1271. <https://doi.org/10.1038/ng.481>
- Sohal, V. S., & Rubenstein, J. L. R. (2019). Excitation-inhibition balance as a framework for investigating mechanisms in neuropsychiatric disorders. *Molecular Psychiatry*, 24(9), 1248–1257. <https://doi.org/10.1038/s41380-019-0426-0>
- Storm, J. F. (1987). Action potential repolarization and a fast after-hyperpolarization in rat hippocampal pyramidal cells. *Journal of Physiology*, 385, 733–759. <https://doi.org/10.1113/jphysiol.1987.sp016517>
- Strupp, M., Teufel, J., Zwergal, A., Schniepp, R., Khodakhah, K., & Feil, K. (2017). Aminopyridines for the treatment of neurologic disorders. *Neurology: Clinical Practice*, 7(1), 65–76. <https://doi.org/10.1212/CPJ.0000000000000321>

- Sudhof, T. C. (2013). Neurotransmitter release: The last millisecond in the life of a synaptic vesicle. *Neuron*, 80(3), 675–690. <https://doi.org/10.1016/j.neuron.2013.10.022>
- Takamori, S., Holt, M., Stenius, K., Lemke, E. A., Grønborg, M., Riedel, D., ... Jahn, R. (2006). Molecular anatomy of a trafficking organelle. *Cell*, 127(4), 831–846.
- Verhage, M., & Sørensen, J. B. (2020). SNAREopathies: Diversity in mechanisms and symptoms. *Neuron*, 107(1), 22–37. <https://doi.org/10.1016/j.neuron.2020.05.036>
- Wheeler, D. B., Randall, A., & Tsien, R. W. (1996). Changes in action potential duration alter reliance of excitatory synaptic transmission on multiple types of Ca²⁺ channels in rat hippocampus. *Journal of Neuroscience*, 16(7), 2226–2237.

SUPPORTING INFORMATION

Additional supporting information may be found online in the Supporting Information section.

How to cite this article: Simmons RL, Li H, Alten B, et al. Overcoming presynaptic effects of VAMP2 mutations with 4-aminopyridine treatment. *Human Mutation*. 2020;1–13. <https://doi.org/10.1002/humu.24109>